Temperature Sensor With Enhanced Sensitivity Based on Photonic Crystal Fiber Interferometer With Material Overlay

Jui-Ming Hsu, Cheng-Ling Lee, Po-Jung Huang, Cheng-Hung Hung, and Pang-Yu Tai

***Abstract*— This letter demonstrates a sensitive photonic crystal fiber interferometer (PCFI) whose sensitivity is enhanced by material dispersion engineering. The interference mechanism in the PCFI originates from the core and cladding modes. Since the cladding modes are strongly influenced by the surroundings, surrounding the PCFI with a material with a high thermo-optic coefficient can greatly improve the temperature sensitivity. The theoretical studies about effective indices of the core and cladding modes in PCF at various temperatures and the interference sensitivity of PCFI with different material surroundings are calculated for comparison with experimental results.**

***Index Terms*— Fiber-optics component, optical fiber sensors, optical interferometry, photonic crystal fiber interferometer (PCFI).**

I. INTRODUCTION

NUMEROUS in-line photonic crystal fiber interferometers (PCFIs) have been extensively used to measure strain ($\mu\varepsilon$) [1], [2], external refractive index (RI) [3], [4], chemical vapor [5], gas pressure [6] and temperature [7]. The structures of PCFIs are generally based on splicing a section of photonic crystal fiber (PCF) between two single-mode fibers (SMFs). The splicing process collapses the air-holes in the PCF cladding, forming a collapsed region with a length of 400–800 μm between the SMF and the PCF. The fundamental mode that is input from the SMF and propagates into the collapsed region can be excited to generate cladding modes that are fed into the PCF. Accordingly, the interference mechanism of the PCFI is almost that between the fundamental and cladding modes (which is typically two-mode interference). The well-known in-line temperature fiber sensors are based on long-period fiber gratings (LPGs) [6], fiber Fabry–Perot interferometers [8], and fiber Mach–Zehnder interferometers [9], and single mode–multimode–single mode (SMS) fiber interferometers [10], [11]. Fiber-based temperature sensors typically have a low temperature sensitivity because silica fiber has an extremely low thermal expansion coefficient (TEC $= +\ 5.5 \times 10^{-7}{}^{\circ}\mathrm{C}^{-1}$) and low thermo-optic coefficient (TOC $= +\ 5 \times 10^{-6}{}^{\circ}\mathrm{C}^{-1}$).

Manuscript received June 15, 2012; revised July 28, 2012; accepted July 30, 2012. Date of publication August 17, 2012; date of current version September 13, 2012.

The authors are with the Department of Electro-Optical Engineering, National United University, Miaoli 360, Taiwan (e-mail: jmhsu@nuu.edu.tw; cherry@nuu.edu.tw; mischa200226@gmail.com; st8005142000@hotmail.com; s100615@yahoo.com.tw).

Color versions of one or more of the figures in this letter are available online at http://ieeexplore.ieee.org.

Digital Object Identifier 10.1109/LPT.2012.2212273

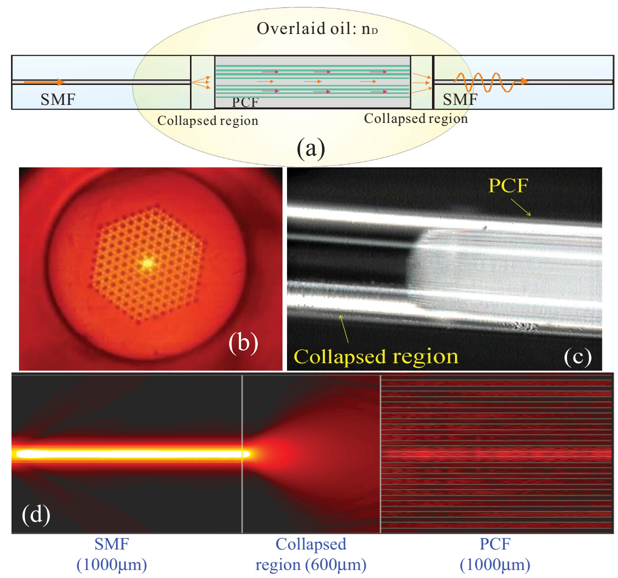

Fig. 1. (a) Configuration of PCFI with engineered material dispersion. (b) Used PCF: LMA-8. (c) Collapsed region in PCFI. (d) Simulation results for field distribution in PCFI with a collapsed region of 600 μm in length.

This letter presents the use of material dispersion engineering to improve the sensitivity of a photonic crystal fiber interferometer (PCFI). Surrounding the PCFI with material can considerably improve its sensitivity to temperature because a PCF interferometer is highly sensitive to index changes, particularly if the index of the external medium is close to that of the cladding [3]. Theory is found to be consistent with experimental results.

Figure 1(a) presents the configuration of the proposed PCFI with material dispersion engineering. Figures 1(b) and (c) shows micrographs of the cross-section and a collapsed region of the PCF (NKT Photonics: LMA-8) that was utilized herein. The collapsed section, in which the air holes in the cladding of the PCF are destroyed, is not an SMF anymore since the waveguide has no cladding. To elucidate the mode expansion in the collapsed region, the field distribution can be simulated using the beam propagation method (BPM), as shown in Fig. 1(d). The fundamental mode is input from the SMF; diffracts in the collapsed region, and then generates cladding modes in the PCF.

II. Theories and Numerical Results

Consider the case in which interference modes are excited and recombined, separately in the two collapsed regions of the interface between the SMF and the PCF. The fundamental SMF mode begins to be diffracted when it enters the collapsed region, as displayed in Fig. 1(d), and excites several cladding modes into the PCF. For a simple intensity-based two-beam interferometer, the visibility of the interference fringes depends on the intensity of the two beams. The interference performance is optimal and the fringe visibility maximal when the intensities of the two beams are equal. In this case, the two interference beams are the fundamental core mode and an excited cladding mode.

The optical phase difference between the two modes is defined as $\Phi = (2\pi/\lambda)\cdot(\mathrm{OPD})$, where OPD is the optical path difference. An accumulated Φ of 2π means that the local tip of the fringe intensity shifts to the next tip. Thus, the wavelengths of two adjacent minima in the spectrum (λ_1 and λ_2) must satisfy the following relation $|\lambda_1 - \lambda_2| = \lambda_1\lambda_2/\mathrm{OPD}$. Here $\mathrm{OPD} = \Delta n_{eff}\cdot L$; L represents the length of the PCF and $\Delta n_{eff} = n_{eff}^{co} - n_{eff}^{cl,x}$, where n_{eff}^{co} and $n_{eff}^{cl,x}$ are the effective indices of the fundamental core mode and the coupling cladding mode of x-th order, respectively. The parameter Δn_{eff} strongly affects the wavelength shift $d\lambda$ because the $d\lambda$ of the proposed PCFI that is associated with a change in temperature (T) can be estimated using the equation

$$\frac{1}{\lambda}\frac{d\lambda}{dT} = \frac{1}{L}\frac{dL}{dT} + \frac{1}{\Delta n_{eff}}\frac{d(\Delta n_{eff})}{dT}. \tag{1}$$

The first term $\frac{1}{L}\frac{dL}{dT}$ is associated with the TEC of the device, and the term $\frac{1}{\Delta n_{eff}}\frac{d(\Delta n_{eff})}{dT}$ is related to the TOC. To identify the sensing mechanism that is described by Eq. (1), a numerical approach is used. The effective indices of the core and five lowest cladding modes of the used LMA-8 PCF are firstly estimated by the plane-wave expansion (PWE) method. From the n_{eff} values of five lowest cladding modes is subtracted the n_{eff} of the fundamental core mode, yielding five groups of $\Delta n_{eff,x}$ (25) and $\Delta n_{eff,x}$(75) values (x: cladding modes 1–5) at 25 °C and 75 °C. The differential terms $d(\Delta n_{eff,x})/dT$ in Eq. (1) can be approximated as the difference values $[\Delta n_{eff,x}(75) - \Delta n_{eff,x}(25)]/\Delta T$. For convenience, an operator $\Theta(\zeta) = \frac{1}{\zeta}\frac{d\zeta}{dT}$ is defined. Figure 2 displays $\Theta(\Delta n_{eff,x})$ for modes 1 to 5.

A negative value of $\Theta(\Delta n_{eff,x})$ in Fig. 2 reveals $\Delta n_{eff,x}$ (75) $<$ $\Delta n_{eff,x}$ (25). According to Eq. (1), in this case, the λ shifts to shorter wavelengths as the temperature increases. In Fig. 2, the value of $\Theta(\Delta n_{eff,x})$ is negative of order 10^{-6}, and its magnitude exceeds that of the positive term $\Theta(L)$, which is of order 10^{-7}. Therefore, the total wavelength shift ($d\lambda$) with the increase in T is negative. The λ is thus determined to shift to a shorter wavelength as the T of the ambient increases. From the calculations, the sensitivity of the $d\lambda$ to T is dominated by the TOC of the PCFI.

In Fig. 2, two special conditions with positive $\Theta(\Delta n_{eff,x})$ apply when modal interference occurs in cladding modes 1 and 2 at $\lambda > 1617$ nm and $\lambda > 1603$ nm, respectively.

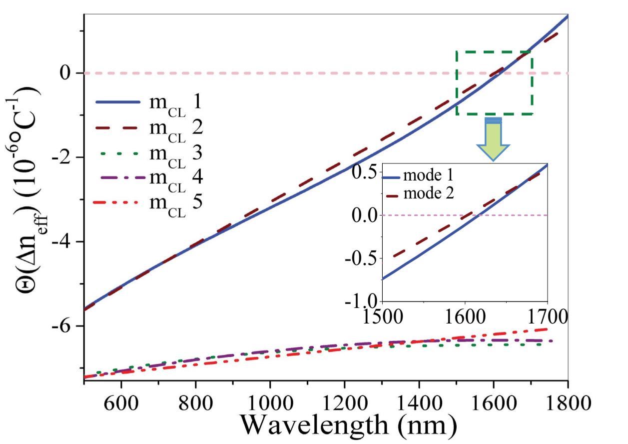

Fig. 2. Calculated $\Theta(\Delta n_{\mathrm{eff},x})$ as a function of wavelength for five lowest groups of Δn_{eff} values. (m_{CL} x) represents the cladding mode of order x.

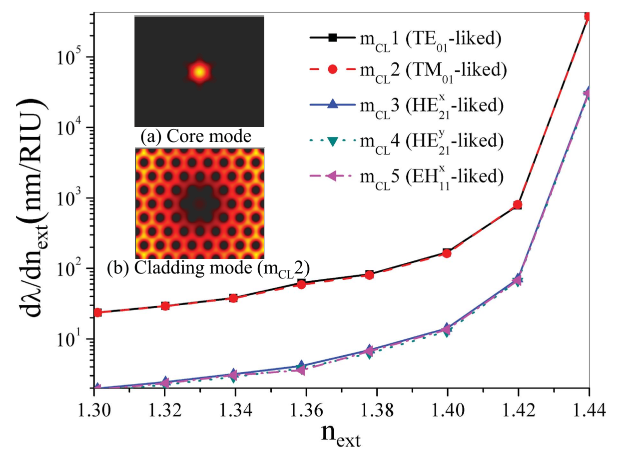

Fig. 3. Dependence of $d\lambda/dn_{ext}$ on surrounding index for five lowest cladding modes. Insets (a) and (b) exhibit the two interference modes.

Accordingly, based on Eq. (1) and the simulated results, $d\lambda$ shifts to shorter wavelengths as T increases, except under the above two conditions.

Since the proposed PCFI is overlaid by a material, its spectral response to a change in external RI is given by [12]

$$\frac{d\lambda}{dn_{ext}} = -\frac{\lambda}{\Delta n_{eff}}\frac{\partial n_{eff}^{cl,x}}{\partial n_{ext}} \Bigg/ \left[1 - \frac{\lambda}{\Delta n_{eff}}\left(\frac{\partial n_{eff}^{co}}{\partial \lambda} - \frac{\partial n_{eff}^{cl,x}}{\partial \lambda}\right)\right]. \tag{2}$$

To study the relationship between the interference pattern and the surrounding RI, the $d\lambda/dn_{ext}$ in Eq. (2) is evaluated using the PWE method again. Figure 3 plots the dependence of $d\lambda/dn_{ext}$ on RI for cladding modes 1~5. These cladding modes resemble the standard TE, TM and hybrid modes of a step-index fiber, the corresponding mode designations are labeled in the legends of Fig. 3. This figure reveals that $d\lambda/dn_{ext} > 0$ for various n_{ext} and all of the modes, indicating that as the temperature increases, the refractive index of the oil decreases and so the interference pattern shifts to shorter wavelengths. In the figure, the $d\lambda/dn_{ext}$ increase (more sensitive) with the surrounding oil index, especially sensitive for the case that the index of the surrounding

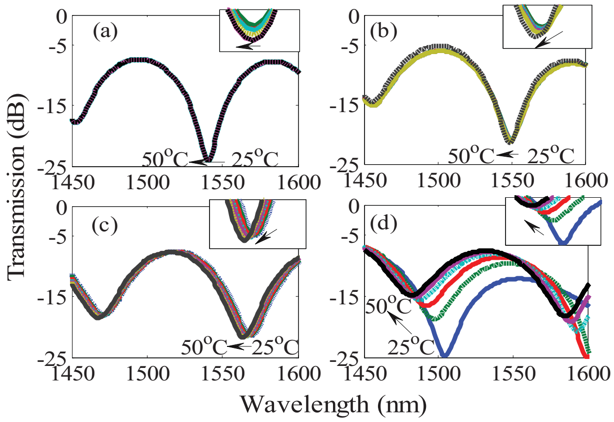

Fig. 4. Experimental transmission spectra of 0.6-cm-long PCFI temperature sensor with various material surroundings (a) in air, (b) $n_D = 1.3$, (c) $n_D = 1.42$, and (d) $n_D = 1.44$.

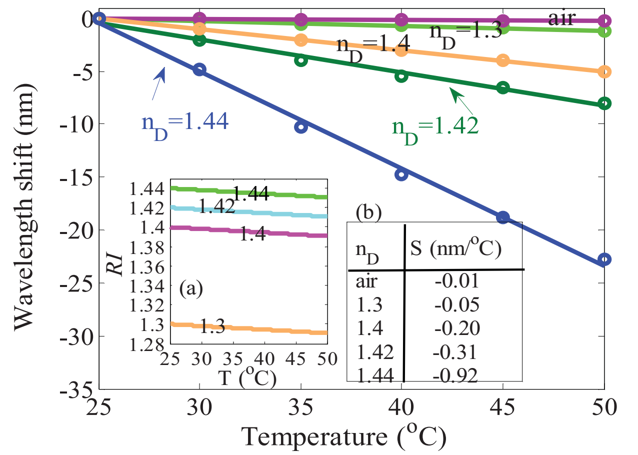

Fig. 5. Sensitivities of shifts in wavelengths of PCFIs with surroundings of various *RI* values. Insets (a) and (b) show *RI* as a function of *T*, and the corresponding sensitivity (*S*) of the used index oil, respectively.

approaches the PCF. It will be deduced from the experimental results in a later paragraphs that the 2nd order cladding mode (the red dashed curve) is the coupling mode that dominates the interference in the proposed PCFI. The insets in Fig. 3 display the mode profiles of the two interference modes.

III. Experimental Results and Discussion

To demonstrate the effectiveness of the proposed PCFI that is overlaid by a material (which is limited at operating temperatures of 20 $\sim$ 70 °C) with a high TOC, transmission spectra are directly obtained using an optical spectrum analyzer (OSA). The applied temperature T(°C) is controlled by a TE cooler from 25 °C to 50 °C to reduce the *RI* of the surrounding liquid (TOC: $dn/dT = -3.74 \times 10^{-4}$ °C^{-1}). Figure 4 presents the transmission spectra thus obtained.

Figure 4 displays the experimental spectra of a PCFI with a PCF length of 0.6 cm that is overlaid with a material of various *RI* values. In air, the proposed PCFI has a very poor sensitivity to external temperature because the pure silica has an extremely low TEC. However, that PCFI with surroundings with an *RI* of $n_D = 1.44$ is sensitive to temperature with a sensitivity of −0.92 nm/°C, which is approximately 92 times that of the same PCFI in air (0.01 nm/°C). This occurs because, at $n_D = 1.44$, the cladding modes greatly stretch out their mode field into the surrounding and are influenced by the surrounding severely. Figure 4 shows that λ hifts to shorter wavelengths as the ambient T increases. In the range of measurement, the experimental results are consistent with the analysis in Section II. Figure 5 plots the fitted linear response of the sensitivities for various *RI*s of the material and the inset (a) plots *RI* as a function of T; the inset (b) lists the relation between n_D and sensitivity in nm/°C. Here, the n_D values of the used Cargille index oil are measured at 25 °C, Sodium D Line, and λ= 589.3 nm. The results reveal a highly linear response to temperature, with high sensitivity when the *RI* of the material approaches that of the fiber, because the cladding modes are strongly stretched out into the surroundings when the *RI* of the material is close to that of the fiber, so the $\Theta(\Delta n_{eff,x})$ varies with great sensitivity to the surrounding.

To look for the coupling cladding mode in the proposed PCFI, it is reasonable for getting λ_1 and λ_2 from the experimental spectrum in Fig. 4(a), and then readily derive the $n_{eff}^{cl,x}$ by using Eq. (1). Comparing the effective indices of the cladding modes with the derived $n_{eff}^{cl,x}$, it is inferred that the two interference modes are the core mode and the second order cladding mode in the presented PCFI.

IV. Conclusion

This letter investigated a sensitive photonic crystal fiber interferometer (PCFI), whose material dispersion was engineered to increase sensitivity to temperature. The spectral responses of the PCFI are strongly influenced by the high thermo-optic coefficient of the overlaid material, improving sensitivity to temperature. Experimental results also revealed that the response of the sensor to temperature was highly linear and, when the *RI* of the material approached that of the fiber, it was highly sensitive.

References

[1] J. Villatoro, V. Finazzi, V. P. Minkovich, V. Pruneri, and G. Badenes, "Temperature-insensitive photonic crystal fiber interferometer for absolute strain sensing," *Appl. Phys. Lett.*, vol. 91, no. 9, pp. 091109-1–091109-3, 2007.

[2] H. Y. Choi, M. J. Kim, and B. H. Lee, "All-fiber Mach–Zehnder type interferometers formed in photonic crystal fiber," *Opt. Express*, vol. 15, no. 9, pp. 5711–5720, 2007.

[3] R. Jha, J. Villatoro, and G. Badenes, "Ultrastable in reflection photonic crystal fiber modal interferometer for accurate refractive index sensing," *Appl. Phys. Lett.*, vol. 93, no. 19, pp. 191106-1–191106-3, 2008.

[4] K. S. Park, H. Y. Choi, S. J. Park, U. C. Paek, and B. H. Lee, "Temperature robust refractive index sensor based on a photonic crystal fiber interferometer," *IEEE Sensors J.*, vol. 10, no. 6, pp. 1147–1148, Jun. 2010.

[5] J. Villatoro, *et al.*, "Photonic crystal fiber interferometer for chemical vapor detection with high sensitivity," *Opt. Express*, vol. 17, no. 3, pp. 1447–1453, 2009.

[6] B. H. Lee, Y. Chung, W. T. Han, and U. C. Paek, "Temperature sensor based on self-interference of a single long-period fiber grating," *IEICE Trans. Electron.*, vol. E83-C, no. 3, pp. 287–292, Mar. 2000.

[7] G. Coviello, V. Finazzi, J. Villatoro, and V. Pruneri, "Thermally stabilized PCF-based sensor for temperature measurements up to 1000 °C," *Opt. Express*, vol. 17, no. 24, pp. 21551–21559, 2009.

[8] Z. Huang, Y. Zhu, X. Chen, and A. Wang, "Intrinsic Fabry–Perot fiber sensor for temperature and strain measurements," *IEEE Photon. Technol. Lett.*, vol. 17, no. 11, pp. 2403–2405, Nov. 2005.

[9] Y. Wang, Y. Li, C. Liao, D. N. Wang, M. Yang, and P. Lu, "High-temperature sensing using miniaturized fiber in-line Mach–Zehnder interferometer," *IEEE Photon. Technol. Lett.*, vol. 22, no. 1, pp. 39–41, Jan. 1, 2010.

[10] L. V. Nguyen, D. Hwang, S. Moon, D. S. Moon, and Y. Chung, "High temperature fiber sensor with high sensitivity based on core diameter mismatch," *Opt. Express*, vol. 16, no. 15, pp. 11369–11375, 2008.

[11] C. L. Lee, K. H. Lin, Y. Y. Lin, and J. M. Hsu, "Widely tunable and ultrasensitive leaky-guided multimode fiber interferometer based on refractive-index-matched coupling," *Opt. Lett.*, vol. 37, no. 3, pp. 302–304, 2012.

[12] T. H. Xia, A. P. Zhang, B. Gu, and J. J. Zhu, "Fiber-optic refractive-index sensors based on transmissive and reflective thin-core fiber modal interferometers," *Opt. Commun.*, vol. 283, no. 10, pp. 2136–2139, 2010.